

# Effect of Fast Fading on Hybrid Detection in VSF-OFCDM Systems

Yiqing Zhou

Dept. of Electrical and Electronic Engineering  
The University of Hong Kong, HONG KONG  
[yqzhou@eee.hku.hk](mailto:yqzhou@eee.hku.hk)

**Abstract**—This paper presents an analytical study on the variable spreading factor (VSF) orthogonal frequency and code division multiplexing (OFCDM) system over a fast fading channel. Hybrid multi-code interference (MCI) cancellation and minimum mean square error (MMSE) detection is proposed in the system as an efficient way to eliminate MCI. It is shown that the optimum power ratio of pilot channel to one data channel is about  $0.25K$ , where  $K$  is the total number of data channels. When the Doppler frequency  $f_D$  is less than 200Hz, the effect of the Doppler on the system performance is negligible. However, increasing  $f_D$  from 200Hz degrades the system performance rapidly. Although the gap in BER between the hybrid and pure MMSE detection decreases as  $f_D$  increases, the gap is still large as long as  $f_D$  is less than around 800Hz. For a wide range of Doppler shift, a larger frequency domain spreading factor ( $N_F$ ) is expected, whereas a smaller time domain spreading factor ( $N_T$ ) provides better performance when  $f_D$  increases.

## I. INTRODUCTION

In future wireless communication systems, a huge bandwidth is needed to support high data rate transmission. An orthogonal frequency and code division multiplexing system (OFCDM) has been proposed for future broadband wireless communications [1]. Based on conventional orthogonal frequency division multiplexing (OFDM), OFCDM systems can combat the severe multi-path interference. Two dimensional spreading with both time and frequency domain spreading is employed in the OFCDM system. The total spreading factor ( $N$ ) is the product of time domain spreading factor ( $N_T$ ) and frequency domain spreading factor ( $N_F$ ), i.e.,  $N = N_T \times N_F$ . Moreover, in order to work in different cell environments, orthogonal variable spreading factor (VSF) is adopted for two-dimensional spreading, and the resultant OFCDM system is called *VSF-OFCDM* system.

Multi-code transmission is employed in the VSF-OFCDM system as an efficient way to achieve high speed transmission. However, in a realistic mobile channel, the code orthogonality no longer remains in time domain because of possible fast fading or in frequency domain because of independent fading among interleaved sub-carriers. In order to improve performance, MCI should be mitigated as much as possible. Hence, the MCI cancellation is considered for the VSF-OFCDM system.

Employing minimum mean square error (MMSE) detection, a hybrid MCI cancellation and MMSE detection scheme is proposed for the VSF-OFCDM system. In the hybrid detection scheme, since the weights of MMSE are

related to the input signal plus interference power, they should be updated stage by stage due to the reduction of MCI after cancellation. The objective of this paper is to analytically investigate the performance of VSF-OFCDM with hybrid MCI cancellation and MMSE detection in a fast fading channel.

The remaining of this paper is organized as follows. Section II introduces the two-dimensional spreading and the system model. Section III presents the theoretical analysis on the performance of the VSF-OFCDM system, while hybrid detection and fast fading are described. Section IV is devoted to discussing the BER for the hybrid detection. Section V presents some representative numerical results. Finally, Section VI draws conclusions.

## II. SYSTEM MODEL

### A. Two Dimensional Spreading

To track the channel variation in a fast fading channel, a code-multiplexed pilot channel is employed. It is one-dimensionally spread only in time domain with the spreading factor  $N_T$ . Without loss of generality, the code with all +1, i.e.,  $C_{N_T}^{(0)}$ , is assigned for the pilot channel. On the other hand, all data channels in VSF-OFCDM are two-dimensionally spread with the total spreading factor  $N = N_T \times N_F$ . The time and frequency domain orthogonal spreading codes are denoted as  $C_{N_T}^{(k_T)} = \{c_{N_T,0}^{(k_T)}, \dots, c_{N_T,N_T-1}^{(k_T)}\}$  and  $C_{N_F}^{(k_F)} = \{c_{N_F,0}^{(k_F)}, \dots, c_{N_F,N_F-1}^{(k_F)}\}$ , respectively. All chips in the codes take +1 or -1. Suppose the  $k^{\text{th}}$  data channel employs the two-dimensional spreading code  $\{C_{N_T}^{(k_T)}, C_{N_F}^{(k_F)}\}$ , then  $k_T = k - \lfloor k/(N_T - 1) \rfloor \cdot (N_T - 1) + 1$  and  $k_F = \lfloor k/(N_T - 1) \rfloor$ , where  $k_T = 1 \sim N_T - 1$ ,  $k_F = 0 \sim N_F - 1$ , and  $\lfloor x \rfloor$  is the integer portion of  $x$ .

For the data channels, assuming that the  $k^{\text{th}}$  data channel with the code  $\{C_{N_T}^{(k_T)}, C_{N_F}^{(k_F)}\}$  is the desired one, the other  $K - 1$  data channels can be divided into two subsets, given by

$$\Omega_A = \{C_{N_T}^{(k_T)}, C_{N_F}^{(k_F)}\}, \hat{k}_F = 0 \sim N_F - 1, \text{ but } \hat{k}_F \neq k_F, k_T \neq 0 \quad (1)$$

$$\Omega_B = \{C_{N_T}^{(\hat{k}_T)}, C_{N_F}^{(\hat{k}_F)}\}, \hat{k}_F = 0 \sim N_F - 1, \hat{k}_T = 1 \sim N_T - 1, \text{ but } \hat{k}_T \neq k_T \neq 0 \quad (2)$$

respectively. The code channels from  $\Omega_A$  are orthogonal to the  $k^{\text{th}}$  data channel only in frequency domain, while code

channels from  $\Omega_B$  must be orthogonal to the  $k^{\text{th}}$  data channel in time domain. Basically, even in a fast fading channel, the MCI in frequency domain is much more serious than in time domain due to independent fading on interleaved sub-carriers. Thus, the time domain spreading should have higher priority than frequency domain spreading. Hence, the number of interfering code channels in  $\Omega_A$  for a desired code channel is at most  $K_A = \lfloor (K-1)/(N_T-1) \rfloor$  and the number of code channels in  $\Omega_B$  is  $K_B = K-1-K_A$ .

### B. System Model

At the transmitter (Fig. 1), information bits on each data channel are first QPSK-modulated, then serial-to-parallel (S/P) converted into  $M/N_F$  streams, where  $M$  is the total number of sub-carriers. Every symbol will be two-dimensionally spread. At the same time, known QPSK-modulated pilot symbols are S/P converted into  $M$  streams, each one of which is spread into  $N_T$  chips in only time domain. Then all data and pilot code channels are combined by a code multiplexer and scrambled. A frequency interleaver is employed to provide frequency diversity. Then, totally  $M$  chips should be up-converted to  $M$  sub-carriers and transmitted in parallel. The IFFT block realizes this operation. After IFFT, an effective OFCDM symbol with  $M$  samples and duration of  $T_s$  is obtained. A guard interval is inserted between OFCDM symbols to prevent inter-symbol interference (ISI). Finally, the complete OFCDM symbol with duration of  $T$  passes through a pulse shaping filter, which gives rise to a transmitted baseband signal.

The receiver block diagram is shown in Fig. 2. With perfect symbol timing, the received equivalent baseband signals are firstly processed by a matched filter. The resultant signals further input to FFT block, which realizes the  $M$ -sub-carrier down conversion. After FFT, the  $M$  obtained chips are deinterleaved and descrambled. On one hand, the output of the descrambler passes through the time domain summation for channel estimation. On the other hand, using the phase information of the estimated channels, the output of the descrambler is weighted by equal gain combining (EGC) and accumulated by the time domain despreader for data channels. When the MCI cancellor is employed, the output from the time domain despreader for data channels is subtracted by a regenerated MCI. After MCI subtraction, signals are multiplied by weights obtained from MMSE algorithms and combined at the frequency domain despreader. QPSK symbols are recovered by a hard decision, parallel-to-serial (P/S) converted and demapped. Finally, information bits at the desired code channel are obtained. The recovered information bits from all other code channels will be used to regenerate the MCI for the desired code channel. Basically, the interference regenerator performs the operation as the transmitter except channel information. This cancellation process will continue in an iterative way until a specified number of stages is reached.

## III. PERFORMANCE ANALYSIS

### A. Transmitted Signal

In forward link, the baseband transmitted signal of the  $m^{\text{th}}$  sub-carrier on the  $i^{\text{th}}$  chip of time domain can be expressed as

$$S(t) = \sum_{m=0}^{M-1} \sum_{i=0}^{N_T-1} [S_{m,i}(t) + S_{p,m,i}(t)] \quad (3)$$

where  $S_{m,i}(t) = \sqrt{P} \sum_{k=0}^{K-1} a_{k,m,i} e^{j2\pi f_m(t-iT)} p(t-iT)$  is the data signal and  $S_{p,m,i}(t) = \sqrt{\beta P} \cdot a_{p,m,i} \cdot e^{j2\pi f_m(t-iT)} p(t-iT)$  is the code multiplexed pilot signal. Here,  $P$  is the signal power on one sub-carrier,  $f_m = m \cdot \Delta f$  is the baseband equivalent frequency of the  $m^{\text{th}}$  sub-carrier and  $a_{k,m,i}$  is the product of data symbol, two-dimensional spreading codes and scrambling code.  $p(t)$  is assumed to be a rectangular pulse with unity amplitude and duration of  $T$ . Furthermore,  $\beta$  is the power ratio of pilot to one data channel and  $a_{p,m,i}$  is the product of pilot symbol, time domain spreading code and scrambling code.

### B. Channel Model and Received Signal

In forward link, all code signals are synchronized and experience the same multi-path fading channel with the low pass equivalent impulse response

$$h(t) = \sum_{l=0}^{L-1} h_l(t) \delta(\tau - \tau_l) \quad (4)$$

where  $h_l(t)$  is the complex time-varying channel fading and  $\tau_l$  is the delay of the  $l^{\text{th}}$  path. When Doppler frequency exists, the autocorrelation function of the  $l^{\text{th}}$  path is defined as

$$\phi_l(\Delta t) = E \{ h_l(t + \Delta t) \cdot h_l^*(t) \} = \sigma_l^2 J_0(2\pi f_D \Delta t) \quad (5)$$

where  $\sigma_l^2 = E \{ |h_l(t)|^2 \}$ ,  $(\cdot)^*$  stands for the conjugate operation,  $f_D$  is the maximum Doppler frequency and  $J_0(\cdot)$  is the zeroth-order Bessel function of the first kind [2].

After experiencing the multi-path channel, the baseband received signal inputs to the matched filter. With ideal symbol timing and no ISI, the output of the matched filter on the  $\hat{m}^{\text{th}}$  sub-carrier in the  $\hat{i}^{\text{th}}$  time chip duration can be expressed as

$$\begin{aligned} r_m(\hat{i}) &= \frac{1}{T_s} \int_{\hat{i}T}^{\hat{i}T+T_s} r(t) \cdot e^{-j2\pi f_m(t-\hat{i}T)} p(t-\hat{i}T) dt \\ &= \sum_{m=0}^{M-1} \left( \sum_{k=0}^{K-1} \sqrt{P} a_{k,m,\hat{i}} + \sqrt{\beta P} a_{p,m,\hat{i}} \right) \cdot \lambda_m^{(m)}(\hat{i}) + N(\hat{m}, \hat{i}) \end{aligned} \quad (6)$$

where  $r(t)$  is the received baseband signal. When  $m = \hat{m}$ ,  $\lambda_m^{(m)}(\hat{i})$  is the factor of interference, whereas when  $m \neq \hat{m}$ ,  $\lambda_m^{(m)}(\hat{i}) = \lambda_m^{(\hat{m})}(\hat{i})$  tends to be the factor of the useful component from the  $\hat{m}^{\text{th}}$  sub-carrier.  $N(\hat{m}, \hat{i})$  is the noise component.

### C. Channel Estimation

In order to demodulate the data signal, the channel estimation is discussed first. The output of the descrambler inputs to the time domain summation for the pilot channel. Actually, the summation is to take simple average of the output of the descrambler over  $\gamma N_T$  chips duration, where  $\gamma$  is an odd integer. Therefore, the resultant output of the summation for pilot is given by

$$r_p(\hat{m}) = \frac{1}{\gamma N_T} \sum_{\hat{i} = (\gamma-1)N_T/2}^{(\gamma+1)N_T/2-1} r_m(\hat{i}) \cdot S_{\hat{m},\hat{i}} \quad (7)$$

Since the pilot symbol is known, the channel estimation for  $N_T$  chips ( $i = 0, 1, \dots, N_T - 1$ ) is given by

$$\bar{\lambda}_{\hat{m}} = \frac{r_p(\hat{m})}{\sqrt{\beta P d_p}} = \frac{1}{\gamma N_T} \sum_{\hat{i}=-\gamma N_T/2}^{(\gamma+1)N_T/2-1} \lambda_{\hat{m}}(\hat{i}) + I_p \quad (8)$$

where  $I_p$  is the total interference plus noise.

Defining the channel estimation error  $e_i = \bar{\lambda}_{\hat{m}} - \lambda_{\hat{m}}(i)$ ,  $i=0 \sim N_T-1$ , the autocorrelation function of  $e_i$  is given by  $R_{err}(i_1, i_2) = E\{e_{i_1} \cdot e_{i_2}^*\}$ . Therefore, the variance of the estimation error,  $e_i$ , is given by  $\sigma_{err}^2(i) = E\{|e_i|^2\} = R_{err}(i, i)$ .

### D. Time Domain Spreading for Data Channels

Suppose the  $\hat{k}^{\text{th}}$  code channel is the desired data channel. A simple EGC is employed in time domain despreading to collect useful signal from different chips. The phase of the channel estimation  $\bar{\lambda}_{\hat{m}}$  is denoted as  $\bar{\varphi}_{\hat{m}}$ . Assuming that the  $\hat{k}^{\text{th}}$  code channel employs two-dimensional spreading code  $\{C_{N_T}^{(k_T)}, C_{N_F}^{(k_F)}\}$ , the signal at the output of the time domain despreader is given by

$$r_{\hat{k}, \hat{m}} = \frac{1}{N_T} \sum_{i=0}^{N_T-1} r_{\hat{m}}(\hat{i}) \cdot e^{-j\bar{\varphi}_{\hat{m}}} \cdot c_{N_T, i}^{(\hat{k}_T)} \cdot s_{\hat{m}, i} \quad (9)$$

### E. Frequency Domain Despreading

In frequency domain despreading, the outputs of the time domain despreader will be weighted by MMSE weights, multiplied by a frequency domain spreading code and then summed over  $N_F$  interleaved sub-carriers. However, in the despreading process, MCI is caused by independent fading on interleaved sub-carriers, so MCI cancellation plus MMSE detection must be employed.

#### E.1. Pure MMSE Detection

The weights of pure MMSE are given by [3]

$$\omega(\hat{m}) = \frac{\hat{\alpha}(\hat{m})}{(1 + K_A) \cdot |\hat{\alpha}(\hat{m})|^2 + \frac{\sigma_{ICL_m}^2}{P} + \frac{\sigma_n^2}{N_T P}} \quad (10)$$

where  $\hat{\alpha}(\hat{m}) = |\bar{\lambda}_{\hat{m}}|$ . For the first symbols on the  $\hat{k}^{\text{th}}$  code channel,  $\hat{m} = m \cdot N_B$  ( $N_B = M/N_F$ ) and  $m = 0 \sim N_F - 1$ . The output of the frequency domain despreader is given by

$$y_{\hat{k}} = \frac{1}{N_F} \cdot \sum_{m=0}^{N_F-1} r_{\hat{k}, m \cdot N_B} \left[ c_{N_F, m}^{(\hat{k}_F)} \cdot \omega(m \cdot N_B) \right] \quad (11)$$

Finally, hard decision will be made on the output,  $y_{\hat{k}}$ , and tentative decision  $d_{\hat{k}}^{(0)}$  will be obtained, where the superscript "0" stands for the 0<sup>th</sup> stage.

#### E.2. Hybrid MCI Cancellation and MMSE Detection

Using the tentative decision from the previous stage, the regenerated MCI at the  $s^{\text{th}}$  stage for the  $(m \cdot N_B)^{\text{th}}$  sub-carrier is given by

$$Q_{m \cdot N_B}^{(s)} = \sqrt{P} \sum_{k \in \Omega_A} d_k^{(s-1)} \cdot c_{N_F, m}^{(k_F)} \cdot \hat{\alpha}(m \cdot N_B) \quad (12)$$

The output of the MCI cancellation is given by

$$r_{\hat{k}, m \cdot N_B}^{(s)} = S_{\hat{k}, m \cdot N_B}^{(s)} + MCI_{m \cdot N_B, A}^{(s)} + MCI_{m \cdot N_B, B}^{(s)} + ICI_{m \cdot N_B}^{(s)} + N_{m \cdot N_B} \quad (13)$$

where  $MCI_{m \cdot N_B, A}^{(s)}$  is the residual MCI, given by

$$MCI_{m \cdot N_B, A}^{(s)} = \sqrt{P} \sum_{k \in \Omega_A} \left[ d_k \cdot \alpha(m \cdot N_B) - d_k^{(s-1)} \cdot \hat{\alpha}(m \cdot N_B) \right] \cdot c_{N_F, m}^{(k_F)} \quad (14)$$

The variance of residual MCI is given by

$$\sigma_{MCI_{m \cdot N_B, A}^{(s)}}^2 \approx 4P \cdot P_b^{(s-1)} \cdot K_A \cdot |\alpha(m \cdot N_B)|^2 + \frac{PK_A}{N_T^2} \sum_{i_1=0}^{N_T-1} \sum_{i_2=0}^{N_T-1} R_{err}(\hat{i}_1, \hat{i}_2) \quad (15)$$

where  $P_b^{(s-1)}$  is the BER of the  $(s-1)^{\text{th}}$  stage.

Therefore, the new weights of MMSE with MCI cancellation can be expressed as:

$$\omega^{(s)}(m \cdot N_B) = \frac{\hat{\alpha}(m \cdot N_B)}{(1 + 4P_b^{(s-1)} K_A) \cdot |\hat{\alpha}(m \cdot N_B)|^2 + \frac{K_A}{N_T^2} \sum_{i_1=0}^{N_T-1} \sum_{i_2=0}^{N_T-1} R_{err}(\hat{i}_1, \hat{i}_2) + \frac{\sigma_{ICL_{m \cdot N_B}}^2}{P} + \frac{\sigma_n^2}{N_T P}} \quad (16)$$

Finally, the output signal of the frequency domain despreader after hybrid detection is expressed as

$$\begin{aligned} y_{\hat{k}}^{(s)} &= \frac{1}{N_F} \sum_{m=0}^{N_F-1} r_{\hat{k}, m \cdot N_B}^{(s)} \left[ c_{N_F, m}^{(\hat{k}_F)} \cdot \omega^{(s)}(m \cdot N_B) \right] \\ &= S_{\hat{k}}^{(s)} + MCI_A^{(s)} + MCI_B^{(s)} + ICI_{\hat{k}}^{(s)} + N \end{aligned} \quad (17)$$

where  $S_{\hat{k}}^{(s)}$  is the desired signal component,  $MCI_A^{(s)}$  is the residual MCI caused by code channels from  $\Omega_A$ ,  $MCI_B^{(s)}$  is the MCI caused by code channels from  $\Omega_B$  and the pilot channel,  $ICI_{\hat{k}}^{(s)}$  is the ICI component and  $N_{\hat{k}}^{(s)}$  is the background noise.

## IV. PERFORMANCE ANALYSIS

When the number of code channels in  $\Omega_B$  is large, conditioned on  $\{\bar{\lambda}_{m \cdot N_B}\}$  and  $\{C_{N_T}^{(k_T)}, C_{N_F}^{(k_F)}\}$ ,  $MCI_B^{(s)}$  in (17) can be modeled as a Gaussian random variable with variance  $\sigma_{MCI_B}^2(s)$ . Therefore, there are three independent Gaussian random variables in  $y_{\hat{k}}^{(s)}$ , i.e.,  $MCI_B^{(s)}$ ,  $ICI_{\hat{k}}^{(s)}$  and  $N_{\hat{k}}^{(s)}$ .

Defining the decision error for the  $k^{\text{th}}$  data channel as  $e_k^{(s-1)} = d_k - d_k^{(s-1)} = e_{I, k}^{(s-1)} + j \cdot e_{Q, k}^{(s-1)}$ , the error probabilities of the real and imaginary parts are supposed be equal and given by  $P(e_{I, k}^{(s-1)} = 0) = 1 - P_b^{(s-1)}$  and  $P(e_{I, k}^{(s-1)} = 1) = P_b^{(s-1)}$ , respectively.

Conditioned on  $\{\bar{\lambda}_{m \cdot N_B}\}$ ,  $\{d_k, k \in \Omega_A\}$  and  $\{e_k^{(s-1)}, k \in \Omega_A\}$ , the conditional error probability at the  $s^{\text{th}}$  stage is given by

$$\begin{aligned} P_b^{(s)} \left( \left\{ \bar{\lambda}_{m \cdot N_B} \right\}, \left\{ d_k \right\}, \left\{ e_k^{(s-1)} \right\}_{k \in \Omega_A} \right) &= \frac{1}{2} \cdot Q \left( \frac{\text{Re} \left( S_{\hat{k}}^{(s)} + MCI_A^{(s)} \right)}{\sigma_{\eta}(s) / \sqrt{2}} \bigg|_{d_{i,i} = d_{0,i} = 1} \right) \\ &+ \frac{1}{2} \cdot Q \left( \frac{\text{Re} \left( S_{\hat{k}}^{(s)} + MCI_A^{(s)} \right)}{\sigma_{\eta}(s) / \sqrt{2}} \bigg|_{d_{i,i} = d_{0,i} = -1} \right) \end{aligned} \quad (18)$$

where  $Q(z) = 1/\sqrt{2\pi} \int_z^{+\infty} e^{-t^2/2} dt$  for  $z \geq 0$ .

In order to obtain the average bit error rate, (18) must be averaged over all conditions. Defining  $\{e_{I, k}^{(s-1)}\}_{n, i}$ ,  $i = 1 \sim \binom{K_A}{n}$ ,

as the  $i^{\text{th}}$  order error vector with  $n$  bit errors, where  $\binom{K_A}{n} = \frac{K_A!}{n!(K_A-n)!}$ , the probability of the  $i^{\text{th}}$  order error vector with  $n$  bit errors out of  $K_A$  codes is given by

$$P(n) = \left(P_b^{(s-1)}\right)^n \cdot \left(1 - P_b^{(s-1)}\right)^{K_A-n} \quad (19)$$

The average of (18) over  $\left\{e_{l,k}^{(s-1)}, k \in \Omega_A\right\}$  is given by

$$\begin{aligned} & P_b^{(s)} \left( \left\{ \bar{\lambda}_{m-N_B} \right\}, \left\{ d_k \right\}, \left\{ e_{Q,k}^{(s-1)} \right\} \Big|_{k \in \Omega_A} \right) \\ &= \sum_{n=0}^{K_A} P(n) \sum_{i=1}^{\binom{K_A}{n}} P_b^{(s)} \left( \left\{ \bar{\lambda}_{m-N_B} \right\}, \left\{ d_k \right\}, \left\{ e_{Q,k}^{(s-1)} \right\}, \left\{ e_{r,k}^{(s-1)} \right\} \Big|_{k \in \Omega_A} \right) \end{aligned} \quad (20)$$

Similarly, the average of (20) over  $\left\{e_{Q,k}^{(s-1)}, k \in \Omega_A\right\}$  is given by

$$\begin{aligned} & P_b^{(s)} \left( \left\{ \bar{\lambda}_{m-N_B} \right\}, \left\{ d_k \right\} \Big|_{k \in \Omega_A} \right) \\ &= \sum_{n=0}^{K_A} P(n) \sum_{i=1}^{\binom{K_A}{n}} P_b^{(s)} \left( \left\{ \bar{\lambda}_{m-N_B} \right\}, \left\{ d_k \right\}, \left\{ e_{Q,k}^{(s-1)} \right\} \Big|_{k \in \Omega_A} \right) \end{aligned} \quad (21)$$

Then (21) should be averaged over all possible  $K_A$  interference data

$$P_b^{(s)} \left( \left\{ \bar{\lambda}_{m-N_B} \right\} \right) = \sum_{j=0}^{4^{K_A}-1} P_b^{(s)} \left( \left\{ \bar{\lambda}_{m-N_B} \right\}, \left\{ d_k \right\}_j \Big|_{k \in \Omega_A} \right) \quad (22)$$

Finally,  $P_b^{(s)} \left( \left\{ \bar{\lambda}_{m-N_B} \right\} \right)$  is averaged over all  $\left\{ \bar{\lambda}_{m-N_B} \right\}$ , which can be numerically evaluated by a Monte Carlo Approach [4].

## V. NUMERICAL RESULTS

Some representative numerical results are presented in this section. A broadband system with 100MHz is employed. Totally,  $M=1024$  sub-carriers are used. The effective OFCDM symbol duration is  $10.24\mu\text{s}$  and the guard interval is set to  $1.76\mu\text{s}$ . Furthermore, the average received signal-to-noise ratio (SNR) per bit is  $SNR_b = 14\text{dB}$  and the system load is defined as  $K/N$ . The times  $\gamma$  of  $N_T$  for channel estimation is set to be  $\gamma=3$ . All the numerical results are based on these assumptions unless noted otherwise.

Fig. 3 illustrates the effect of power ratio  $\beta$  on the performance of a two-dimensionally spreading system with various system loads. The Doppler shift  $f_D$  is 500Hz. It can be seen from the figure that when  $\beta$  is small, the system performance degrades by the poor channel estimation. When  $\beta$  increases, BER performance improves as the quality of channel estimation improves, and BER reaches a minimum for a particular value of  $\beta$ . Further increasing  $\beta$  beyond that value increases BER due to the low transmit power efficiency and more interference caused to data channels by the pilot channel. When the system load is  $K/N = 0.25$ , the optimum  $\beta$  is around 12dB. However, when system load is  $K/N = 0.75$ , the optimum  $\beta$  is around 18dB. Generally speaking, the optimum  $\beta$  can be set to be about 25% of the total number of data channels, i.e.,  $\beta = 0.25K$ . Moreover, the significant improvement in BER performance can be achieved by making use of the hybrid detection. For either heavy or light system load, the most significant reduction in BER is obtained by the

1-stage hybrid detection, then the improvement decreases when the number of stages increases. For the light load, a 1-stage hybrid detector is sufficient, whereas for the heavy load, 2-stage hybrid detection is necessary.

The BER is plotted in Fig. 4 as a function of  $f_D$  with  $N = 16 \times 16$ ,  $K/N = 0.75$ , and  $\beta = 0.25K$  for pure MMSE, 1-stage, 2-stage and 3-stage hybrid, respectively. It can be seen from the figure that when  $f_D$  is small ( $f_D \leq 200\text{Hz}$ ), the performance of each detection is very stable and the performance of the hybrid is much better than that of the pure MMSE. Considering 2-stage hybrid is sufficient. When  $f_D$  increases from 200Hz, the performance of any detection degrades dramatically due to poor channel estimation. Furthermore, the degradation in performance is much rapid for hybrid than for pure MMSE. This is because when  $f_D$  increases, MCI in time domain increases, which cannot be cancelled out by the hybrid detection. When  $f_D$  becomes large ( $f_D \geq 1000\text{Hz}$ ), the BER performances of the pure MMSE and hybrid detection are approaching closely. In general, as long as  $f_D$  is less than 800Hz, improvement in BER with hybrid detection is still significant.

The BER of the 2-stage hybrid is plotted in Fig. 5 as a function of  $N_F$  for various values of  $f_D$ . For similar channel estimation,  $\gamma$  is assumed to be 3 and 5 for  $N_T = 16$  and  $N_T = 8$ , respectively. It can be seen that for a given  $f_D$  when  $N_F$  increases, the system performance improves. This is because with hybrid detection, when  $N_F$  increases, the frequency diversity gain increases and overcomes the increased MCI in frequency domain. Note that for  $N_T = 16$  and  $f_D = 1000\text{Hz}$ , the system performance degrades slightly when  $N_F$  increases from a small value and keeps stable. Furthermore, when  $f_D$  is small, the performance difference between  $N_T = 16$  and  $N_T = 8$  is negligible. However, the difference increases with  $f_D$ . When  $f_D \geq 500\text{Hz}$ , the system with  $N_T = 8$  performs much better than that with  $N_T = 16$ . This is because the MCI in time domain is larger with  $N_T = 16$ . This MCI increases with  $f_D$  and cannot be cancelled out by the hybrid detection. In summary, with similar channel estimation quality, a larger frequency domain spreading factor is preferred, irrespective of the Doppler shift  $f_D$ . But a shorter  $N_T$  is more favorable when  $f_D$  increases.

## VI. CONCLUSIONS

An analytical study is presented in this paper on the effect of fast fading on performance of the VSF-OFCDM system with hybrid MCI cancellation and MMSE detection. The following conclusions are drawn:

- 1) The optimum power ratio ( $\beta$ ) between pilot and one data channel takes a value around  $0.25K$  for a wide range of the systems load.
- 2) The hybrid detection outperforms the pure MMSE. 1-stage hybrid is sufficient when the system load is light whereas 2-stage hybrid is necessary for heavy system loads.
- 3) When the Doppler frequency  $f_D < 200\text{Hz}$ , the effect of the Doppler on the system performance can be negligible. When  $f_D < 800\text{Hz}$ , the hybrid detection still provides significant improvement in performance compared to the pure MMSE detection.

4) In order to achieve good performance for a wide range of Doppler shifts, a larger  $N_F$  is preferred, while a shorter  $N_T$  should be employed, especially when Doppler frequency is high.

**ACKNOWLEDGEMENT**

The author would like to thank Dr. M. Sawahashi, Dr. K. Higuchi, Dr. H. Atarashi and Dr. J. Wang for their helpful discussions.

**REFERENCES**

- [1] H. Atarashi and M. Sawahashi, "Investigation of inter-carrier interference due to Doppler spread in OFCDM broadband packet wireless accesses," *Special issue on software defined radio technologies and its applications*, 2002SRP-28.
- [2] W. C. Jakes, "Microwave mobile communications," Piscataway, N.J.: IEEE Press, 1993.
- [3] J. P. Linnarz, "Performance analysis of synchronous MC-CDMA in mobile rayleigh channel with both delay and Doppler spreads," *IEEE Trans. on Vehicular Technology*, vol. 50, no. 6, Nov. 2001.
- [4] Zhou Xing, "Parallel ensemble Monte Carlo for device simulation," *Workshop on High Performance Computing Activities in Singapore*, National Supercomputing Research Center, Sept. 1995.

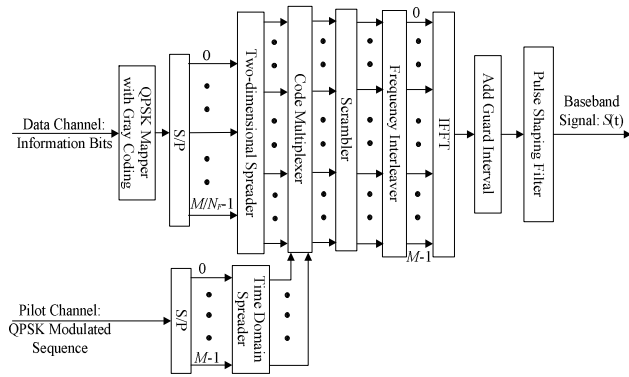


Figure 1. Transmitter block diagram of the VSF-OFCDM system

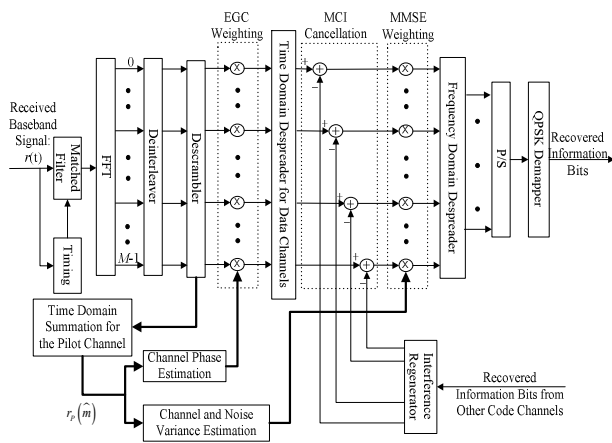


Figure 2. Receiver block diagram of the VSF-OFCDM system with hybrid MCI cancellation and MMSE detection

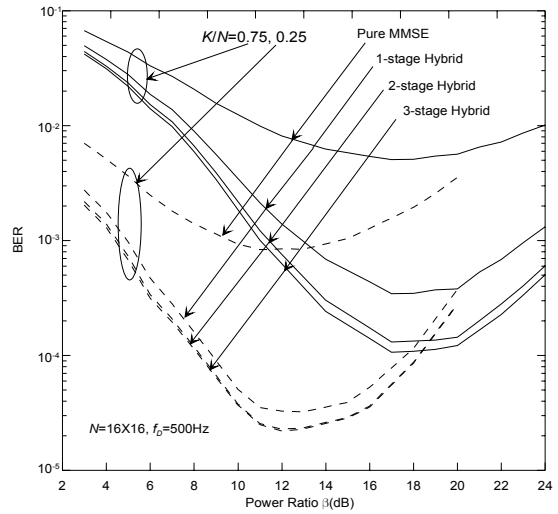


Figure 3. System performance as a function of  $\beta$

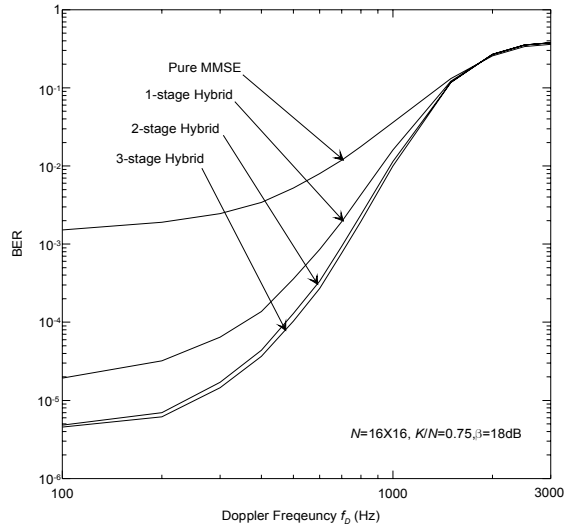


Figure 4. Performance of hybrid detection as a function of Doppler frequency

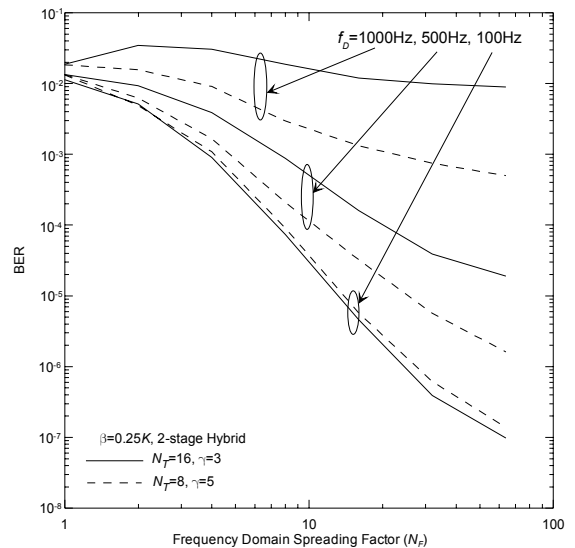


Figure 5. System performance as a function of  $N_T$